



USP13 inhibition exacerbates mitochondrial dysfunction and acute kidney injury by acting on MCL-1

Qian Wang^{a,b,c,d}, Shihan Cao^{a,b,c}, Zhenzhen Sun^{a,b,c}, Wenping Zhu^{a,b,c},
Le Sun^{a,b,c}, Yuanyuan Li^f, Dan Luo^g, Songming Huang^{a,b,c}, Yue Zhang^{a,b,c,*},
Weiwei Xia^{a,b,c,e,*}, Aihua Zhang^{a,b,c,*}, Zhanjun Jia^{a,b,c,*}

^a Department of Nephrology, Children's Hospital of Nanjing Medical University, Nanjing, China

^b Nanjing Key Laboratory of Pediatrics, Children's Hospital of Nanjing Medical University, Nanjing, China

^c Jiangsu Key Laboratory of Pediatrics, Nanjing Medical University, Nanjing, China

^d Department of Cardiology, Children's Hospital of Nanjing Medical University, Nanjing, China

^e Department of Clinical Laboratory, Children's Hospital of Nanjing Medical University, Nanjing, China

^f Department of Endocrinology, Children's Hospital of Nanjing Medical University, Nanjing, China

^g Department of Nephrology, Shunde Hospital of Southern Medical University, Foshan, China

ARTICLE INFO

Keywords:

USP13

MCL-1

Mitochondrial dysfunction

Acute kidney injury

Deubiquitination

ABSTRACT

Acute kidney injury (AKI) is a globally recognized public health issue that lacks satisfactory therapeutic strategies. Deubiquitinase ubiquitin-specific protease 13 (USP13) regulates various pathophysiological processes via the deubiquitination of multiple substrates. However, its role in AKI remains unclear. To illustrate the role and underlying mechanism of USP13 in AKI, we subjected *Usp13* knockdown mice, and mice treated with the USP13 inhibitor spautin-1, and mice with USP13 overexpression plasmids to cisplatin challenge. Renal tubular epithelial cell injury and mitochondrial disturbances were determined in vitro. Immunoprecipitation and deubiquitylation assays were performed to verify the interactions between USP13 and myeloid cell leukemia (MCL-1). We observed a significant decrease of USP13 expression in cisplatin-challenged AKI mice and renal tubular epithelial cells. Overexpression of USP13 alleviated kidney injury, whereas knockdown or inhibition of USP13 further exacerbated AKI. Mechanistically, USP13 downregulation resulted in increased degradation of MCL-1 which is a key regulator of cell survival and mitochondrial function, and the resultant MCL-1 reduction disrupted mitochondrial homeostasis and aggravated renal tubular epithelial cell injury and death, contributing to AKI progression. In conclusion, our findings demonstrated that inhibition of USP13 could exacerbate mitochondrial dysfunction and AKI through its effects on MCL-1, and USP13 may serve as a target for AKI prevention and treatment.

1. Introduction

Acute kidney injury (AKI) is a common disease with a dramatic decline in renal function in a short period [1,2]. Etiologies of AKI include toxins, drugs, ischemia, hypoxia, infections, trauma, and operations [3,4]. Nephrotoxicity is the most common adverse effect observed in patients receiving cisplatin chemotherapy. AKI can develop into acute renal failure, which requires continuous renal replacement therapy, and places a significant financial burden on families and society [5]. In addition, the mechanism of AKI occurrence is complex, and there is currently no specific targeted therapy available. Therefore, an in-depth

exploration of the molecular mechanisms of AKI and the search for novel targets for intervention may provide novel insights for the prevention and treatment of clinical AKI.

Ubiquitin-specific protease 13 (USP13) is a member of the deubiquitinases (DUBs) family and plays vital roles in a variety of pathophysiological processes by removing ubiquitin from substrates, including the cell cycle, DNA damage repair, neurodegeneration, and tumorigenesis [6,7]. Previous studies revealed that USP13 could positively regulate the cell cycle and DNA damage repair while served as a negative regulator in the pathogenesis of neurodegenerative diseases [8–10]. The role of USP13 in tumorigenesis is still controversial, for

* Corresponding authors at: Department of Nephrology, Children's Hospital of Nanjing Medical University, Nanjing, China.

E-mail addresses: zyflora2006@hotmail.com (Y. Zhang), xiawwpku@163.com (W. Xia), zhaihua@njmu.edu.cn (A. Zhang), jiazj72@hotmail.com (Z. Jia).

<https://doi.org/10.1016/j.bbadis.2024.167599>

Received 9 August 2024; Received in revised form 24 November 2024; Accepted 24 November 2024

Available online 27 November 2024

0925-4439/© 2024 Elsevier B.V. All rights reserved, including those for text and data mining, AI training, and similar technologies.

most studies supported USP13 as an oncogenic factor owing to its deubiquitination and stabilization of multiple carcinogenic factors while the tumor suppressor phosphatase and tensin homolog was also recognized as a substrate of USP13 [11–13]. Currently, little research has been conducted on the role of USP13 in renal diseases. In kidney cancers, USP13 stabilized the zinc fingers and homeoboxes 2 (ZHX2) to facilitate renal cell carcinoma progression [14]. Recently, a study reported that the anti-tumor drug nilotinib-induced USP13 downregulation failed to stabilize Bcl-xL and the reduction in Bcl-xL levels led to mitochondrial damage and apoptosis activation, thereby accelerating kidney injury and fibrosis [15]. However, no study has elucidated the role of USP13 in AKI.

Recent studies have described deubiquitination of myeloid cell leukemia (MCL-1) by USP13 [16]. MCL-1 is an important anti-apoptotic factor in B-cell lymphoma-2 (BCL-2) family, and is widely distributed in various tissues and cells [17,18]. Numerous studies have shown the high expression of MCL-1 in various tumor types and promotes tumor progression by inhibiting cell apoptosis [19]. In addition to promoting tumorigenesis, the anti-apoptotic effect of MCL-1 is vital for early erythropoiesis [20], cell survival [21–24], and nervous system development [25]. Notably, MCL-1 is indispensable for maintaining mitochondrial structure and function. Mice lacking the *Mcl-1* gene in cardiomyocytes have been shown to spontaneously develop fatal dilated cardiomyopathy accompanied by mitochondrial structural abnormalities and respiratory defects [26,27]. Other studies have also highlighted the necessity of MCL-1 for ATP production, mitochondrial respiration, mitochondrial dynamics, and maintenance of mitochondrial ridge structures [28–30]. These investigations suggest an irreplaceable role for MCL-1 in maintaining normal mitochondrial homeostasis.

Mitochondria are energy supply factories and are particularly important for cells with high energy requirements, such as renal tubular epithelial cells. However, mitochondria are extremely susceptible to various stimuli such as toxins, ischemia, and hypoxia. Mounting evidence has revealed that mitochondrial dysfunction, including oxidative stress, impaired mitophagy, mitochondrial DNA (mtDNA) damage, and metabolic disorders, is closely associated with AKI [31–34]. Many studies, our previous work included, have demonstrated that impaired mitochondrial function further advances AKI, whereas restoring mitochondrial function can significantly alleviate kidney injury [35–38].

In the present study, cisplatin- and folic acid (FA)-treated mice and tubular epithelial cells were utilized to explore the role of the USP13/MCL-1 axis in AKI. We demonstrated that USP13/MCL-1 was down-regulated in AKI, and high-expression of USP13 or MCL-1 mitigated kidney injury, whereas gene knockdown or pharmacological inhibition of USP13 exacerbated the progression of kidney injury by disrupting mitochondrial function and promoting cell death. Our data provides a potential strategy for targeting USP13/MCL-1 to prevent and treat AKI.

2. Materials and methods

2.1. Chemical and reagents

Cisplatin (H20023461) was purchased from Qilu Pharmaceutical (Shandong, China), and spautin-1 (HY-12990) was obtained from MedChemExpress (Shanghai, China). The TdT mediated dUTP nick end labeling (TUNEL) staining kit (A112-02) was obtained from Vazyme (Nanjing, China). Thermo Fisher Scientific (Waltham, MA, USA) supplied Tetramethylrhodamine methyl ester (TMRM) (I34361) and Mito-SOX (M36008) kits. Annexin V-FITC Apoptosis Detection Kit was obtained from BD Biosciences (New Jersey, USA). Primary antibodies against USP13 (Cat No. 16840, Cat No. 66176), MCL-1 (Cat No. 16225), BCL-2 (Cat No. 26593), optic atrophy protein (OPA1) (Cat No. 27733), GAPDH (Cat No. 60004), β -actin (Cat No. 66009), LaminB1 (Cat No.12987), and HA (Cat No.51064) were acquired from Proteintech (Wuhan, China). Antibodies against neutrophil gelatinase-associated lipocalin (NGAL) (Ab63929), translocase of outer mitochondrial

membrane 20 (TOM20) (Ab56783), and dynamin-related protein 1 (DRP1) (Ab184247) were obtained from Abcam (Cambridge, UK). The kidney injury molecule 1 (KIM-1) antibody (AF1817) was provided by R&D Systems (Minneapolis, MN, USA), and the FLAG antibody (F1804) was supplied by Sigma-Aldrich (St. Louis, Missouri, USA).

2.2. Human specimens

Human research protocols got approval from the Children's Hospital of Nanjing Medical University Medical Ethical Committee and in accordance with declaration of Helsinki. All patients signed a written informed consent form. Four kidney biopsy samples were obtained from AKI patients admitted to the Department of Nephrology, Children's Hospital of Nanjing Medical University. Five para-carcinoma kidney biopsy samples from patients who underwent partial nephrectomy for benign renal tumors were used as normal controls. AKI diagnosis was made based on the KDIGO criteria. Table S1 shows the clinical parameters of AKI patients.

2.3. Animal studies

All animal experiments complied with ARRIVE guidelines and were carried out based on the principles formulated by the National Ministry of Science and Technology of China. The experimental protocols received approval from the Animal Ethics Review Committee of Nanjing Medical University.

Wild-type (WT) mice and *Usp13* heterozygous (Het) mice with a C57BL/6N background were obtained from GemPharmatech (Nanjing, China) and raised in a pathogen-free animal facility. They were kept under a 12:12 h light/dark cycle with eating and drinking ad libitum. We conducted all our animal experiments at the Animal Research Center of Nanjing Medical University and all experimental protocols got approval from the Institutional Animal Care and Use Committee of Nanjing Medical University (2407058).

Three experiments were performed to elucidate the role of USP13 in cisplatin-induced AKI. First, we divided *Usp13* Het and WT mice into four groups: WT + Saline, WT + Cis, Het + Saline, and Het + Cis. These mice were injected with an equal amount of saline or cisplatin (25 mg/kg) intraperitoneally. Three days later, we euthanized the mice and collected blood and kidney tissues for measurements. Second, USP13 was overexpressed in the kidneys of mice through tail vein injection of USP13 plasmids. Mice received 80 μ g scrambled or USP13 plasmids dissolved in 2 mL of saline, administered via high pressure injection within 5–10 s. After 36 h, cisplatin was intraperitoneally administered to induce kidney injury. Third, a USP13 inhibitor, spautin-1 (10 mg/kg), was pre-administered to mice via intraperitoneal injection 1 day before cisplatin treatment and continued once daily for the following 3 days until the mice were euthanized.

To verify the role of USP13 in AKI, we also conducted FA-induced mice model. Mice were divided into two groups: WT + FA and Het + FA; they were treated with FA (250 mg/kg) via a single intraperitoneal injection or an equal amount of sodium bicarbonate. After 24 h, these mice were euthanized.

To investigate the role of MCL-1 in cisplatin-AKI, MCL-1 or scrambled plasmids (80 μ g/per mouse) were used to overexpress MCL-1 in mouse kidney tissues via tail vein injection. After 36 h, cisplatin was intraperitoneally injected to induce AKI. After 3 days, the mice were euthanized, and blood and kidney tissues were harvested.

2.4. Serum biochemistry analysis

Blood samples were collected and serum was obtained via centrifugation at 3000 rpm for 20 min. Serum creatinine (Cr) and blood urea nitrogen (BUN) levels were determined by an automatic biochemistry analyzer, and serum cystatin C (Cys C) concentrations were determined with an ELISA kit.

2.5. Histology

Mouse kidney tissues were sequentially fixed in 4 % paraformaldehyde overnight, dehydrated using a tissue dehydrator, and embedded in paraffin. Periodic acid-schiff (PAS) staining (G1281, Solarbio, China) was performed in 3 μ m thick slices following the manufacturer's instructions. Under a microscope, the sections were examined and scored based on the degree of pathological damage: 0 (normal), 1 (<25 % damage), 2 (25 %–50 % damage), 3 (50 %–75 % damage), and 4 (>75 % damage).

2.6. TdT mediated dUTP nick end labeling staining

Kidney cell apoptosis was examined utilizing a TUNEL BrightGreen Apoptosis Detection Kit (A112-02), according to the manufacturer's instructions. A confocal microscope (LSM710; Carl Zeiss, Germany) was used to capture apoptotic cells showing green fluorescence. At least five randomly selected non-overlapping fields were counted for each sample.

2.7. Immunohistochemistry

Immunohistochemistry (IHC) staining was performed using an IHC detection kit (ZSGB-BIO, PV-9000) following the manufacturer's instructions. 3 μ m kidney slides were deparaffinized before antigen retrieval. Then the slides were incubated in 3 % hydrogen peroxide for 10 min, washed three times with PBS, and blocked with 5 % goat serum for 1 h before incubating with primary antibodies (dilution rate, 1:200) at 4 °C overnight. On the second day, after incubation with the reaction enhancer for 20 min, peroxidase-conjugated secondary antibodies were added and incubated for 1 h at room temperature, followed by DAB staining. Images were captured using an Olympus microscope, and the signals were analyzed using ImageJ software (Wayne Rasband, USA).

2.8. Immunofluorescence

The protocol for immunofluorescence (IF) of kidney tissues was similarly to that for IHC, with the key difference being the addition of TritonX-100 for increased permeability. The IF protocol for the cells is as follow. Mouse proximal tubular cells (mPTCs) cultured in the glass-bottomed cell culture dishes (Cat No. 801001, NEST, China) were washed, fixed, permeabilized with PBS + 0.5 % TritonX-100 for 20 min and then blocked with blocking solution (PBS + 0.3 % TritonX-100 + 5 % goat serum) for 1 h. The primary antibodies were diluted (dilution rate: 1:50) in PBS + 1 % BSA + 0.3 % TritonX-100 and incubated overnight at 4 °C. On the second day, the cells were washed and incubated with secondary antibodies (dilution rate: 1:500) for 1 h in the dark. Finally, after nuclear staining with DAPI, the cells were observed and photographed under a confocal microscope.

2.9. Cell culture and treatment

mPTCs (also named TKPT, CVCL_UJ13) were obtained from American Type Culture Collection (Manassas, VA) through Beijing Zhongyuan Heju Biotechnology (Beijing, China). HK-2 cells (CVCL_0302) were obtained from FuHeng Biology (Shanghai, China) and HEK293T cells (CVCL_0063) were provided by Zhong Qiao Xin Zhou Biotechnology (Shanghai, China). These cells were cultured in DMEM/F-12 or DMEM medium (Wisent, Canada) containing 10 % fetal bovine serum (PAN, Germany) and 1 % penicillin/streptomycin in an atmosphere of 5 % CO₂ at 37 °C. USP13 or MCL-1 plasmids or siRNA were transfected to the cells via lipo2000 (11668-019, ThermoFisher, USA) according to the manufacturer's instructions with or without cisplatin (5 μ g/mL) treatment for 24 h. Mouse USP13 and MCL-1 plasmids were synthesized by the Public Protein/Plasmid Library (PPL, China). Mouse/human USP13 and mouse Mcl-1 siRNAs were obtained from RIBOBIO (Guangzhou, China) with the following sequences: mouse *Usp13* siRNA:

GTATCGAAGTATGCCAACA; human *USP13* siRNA: CAATGAGTGGT-CATTACAT; mouse *Mcl-1* siRNA: CCACGTACAGGACCTAGAA.

2.10. Cell viability assay

A CCK-8 assay kit (KGA317, KeyGen Biotech, China) was used to detect the cell viability. The mPTCs were seeded into 96-well plates. After the corresponding treatments, the cells were incubated with CCK8 working solution (10 μ L CCK-8 reagent for each well) for 1–2 h. A Multiskan FC microplate reader (Thermo Fisher Scientific, USA) was utilized to measure the absorbance of cells at 450 nm.

2.11. Annexin V/PI staining

An apoptosis detection kit (556,547, BD Biosciences, USA) was used to detect cell apoptosis in vitro. After treatments, the mPTCs were washed, trypsinized with EDTA-free trypsin, centrifuged (1000 rpm, 5 min), and stained with Annexin V-FITC and PI according to the manufacturer's instructions. After 15 min of incubation in the dark at room temperature, a flow cytometer (BC50403, Beckman, USA) was used to measure the fluorescence intensity.

2.12. Mitochondrial membrane potential (MMP) and mitochondrial reactive oxygen species (mitoROS)

The MMP and mitoROS of mPTCs were detected with TMRM (I34361, ThermoFisher, USA) and MitoSOX (M36008, ThermoFisher, USA), respectively, following the manufacturer's instructions. After treatments, the mPTCs were incubated with TMRM or MitoSOX for 30 or 10 min respectively at 37 °C in the dark. A flow cytometer was utilized to measure the fluorescence intensity.

2.13. Measurement of ATP content

The ATP content in mPTCs was determined utilizing an Enhanced ATP Assay Kit (S0027, Beyotime, China) following the manufacturer's instructions. The relative light unit values were determined and calculated with a GloMax® 96 Microplate Luminometer (Promega, USA).

2.14. Seahorse analysis of cell oxygen consumption rate (OCR)

The mPTCs were seeded into 96-well plates and transfected with USP13 siRNA. After 24 h, a Seahorse XF96 Extracellular Flux Analyzer (Agilent Technologies, CA, USA) was used to measure the OCR. The medium was replaced with Seahorse assay medium 1 h before detection. The ATP synthase inhibitor oligomycin (1 mM), the uncoupler carbonyl cyanide 4- trifluoromethoxy-phenylhydrazine (1 μ M), and a mixture of the complex I inhibitor rotenone (0.5 μ M) and complex III inhibitor antimycin A (0.5 μ M) were successively added to the cells, and OCR was measured at different time points. The basal and ATP-linked respiration levels were also calculated.

2.15. Co-immunoprecipitation

USP13-Flag or MCL-1-Flag plasmids were transfected into 293T cells, while USP13-Flag+MCL-1-HA plasmids were transfected into mPTCs. Both cell types were treated with the protease inhibitor MG132 (10 μ M) (HY13259, MCE, China) for 8 h before collection. The cells were lysed on ice using cell lysis buffer (P0013, Beyotime, China) supplemented with a protease inhibitor cocktail (04693132001, Roche, Basel, Switzerland) and a phosphatase inhibitor cocktail (04906845001, Roche, Basel, Switzerland). The prewashed protein A/G magnetic beads were premixed with the whole-cell lysate and placed on a Ferris wheel-type rotary mixer for 1–2 h to remove non-specific binding. Next, the beads were discarded, and then the 293T cell lysates were mixed with mouse anti-Flag antibody (10 μ g/mL) and normal mouse IgG.

Meanwhile, the mPTCs lysates were combined with rabbit anti-USP13 or rabbit anti-MCL-1 antibodies, along with rabbit IgG, and rolled for 2 h at 4 °C. Subsequently, the newly processed beads, whole cell lysates, and antibodies were mixed and incubated overnight at 4 °C. On the second day, after the beads were washed, 1 × SDS loading buffer (P0015A, Beyotime, China) was used to elute the samples, and western blotting was performed to detect the interaction between proteins.

2.16. Western blotting

Kidney tissues, mPTCs, and HK2 cells were lysed using RIPA buffer (P0013K, Beyotime, China) containing a protease inhibitor cocktail. The supernatant was collected from the lysed cells via centrifugation at 12000 rpm for 15 min, and a BCA Protein Assay Kit (P0012, Beyotime, China) was utilized to determine the concentration of the samples. Approximately 30–50 µg protein samples were loaded and separated on SDS-PAGE gels, and then transferred onto PVDF membranes. Next, 5 % nonfat milk was applied for blocking the PVDF membranes at room temperature for 1 h. The primary antibodies (dilution rate: 1:1000) were incubated with the PVDF membranes at 4 °C overnight. On the next day, the corresponding secondary antibodies (dilution rate: 1:5000) were incubated with the PVDF membranes for 1 h at room temperature. An enhanced chemiluminescence detection system (Bio-Rad, Hercules, CA, US) was used to determine the expression of target proteins. Densitometric analysis was conducted utilizing the ImageJ software.

2.17. Real-time quantitative polymerase chain reaction (RT-qPCR)

TRIzol reagent (Invitrogen, Carlsbad, CA, USA) was used to extract RNA from the kidney tissues, mPTCs and HK2 cells. RNA concentration was determined with a NanoDrop One spectrophotometer (Thermo Fisher Scientific). Then, a HiScript II Q RT SuperMix for qPCR (Vazyme, Nanjing, China) was employed to reverse transcribe RNA to cDNA. RT-qPCR system was prepared utilizing a SYBR Green Premix Kit (Vazyme, Nanjing, China) and conducted on a Roche LightCycler 96 system (Roche, Switzerland). Table S2 listed the primer sequences. GAPDH or 18s was used as the internal control.

2.18. Statistical analysis

Statistical analyses were performed utilizing the GraphPad Prism 8 software (La Jolla, CA, USA). Data are presented as the mean ± SEM. Student's *t*-test or one-way ANOVA was used for statistical analysis. *P* < 0.05 was considered statistically significant.

3. Results

3.1. USP13 was downregulated in AKI

First, we performed immunofluorescence staining to observe the localization and expression of USP13 in normal human and mouse kidneys. Colocalization of USP13 and *lotus tetragonolobus* lectin (LTL), a marker of proximal tubules, confirmed USP13 expression in renal tubular epithelial cells (Fig. 1A). We then examined USP13 expression in kidney biopsy samples from AKI patients. Fig. 1B showed a marked reduction in USP13 expression in the kidney tissues of AKI patients, compared to that in the normal controls (Fig. 1B). Simultaneously, we also observed decreased USP13 expression in cisplatin-treated mouse kidneys, as evidenced by immunohistochemical and western blotting analyses (Fig. 1C, D). Consistently, in mouse renal epithelial cells treated with cisplatin, USP13 was also markedly downregulated (Fig. 1E). The reduction in USP13 levels may contribute to or inhibit AKI progression.

3.2. USP13 knockdown aggravated cisplatin- and FA-induced AKI

During the mice breeding, we observed a severe impact of homozygous *Usp13* KO on the fertility. Thus, to investigate the role of USP13 in AKI, we performed experiments using *Usp13* het mice. In this study, we subjected *Usp13* het mice to cisplatin treatment (25 mg/kg, 72 h) to induce AKI (Fig. 2A). In mice treated with cisplatin, serum BUN and Cys-C levels were significantly higher in Het mice than in WT mice (Fig. 2B). Moreover, USP13 knockdown aggravated cisplatin-induced pathological kidney damage (tubular dilation, brush border loss, and cast formation), as determined through PAS staining (Fig. 2C). In addition, the levels of the tubular injury marker proteins NGAL and KIM-1 were

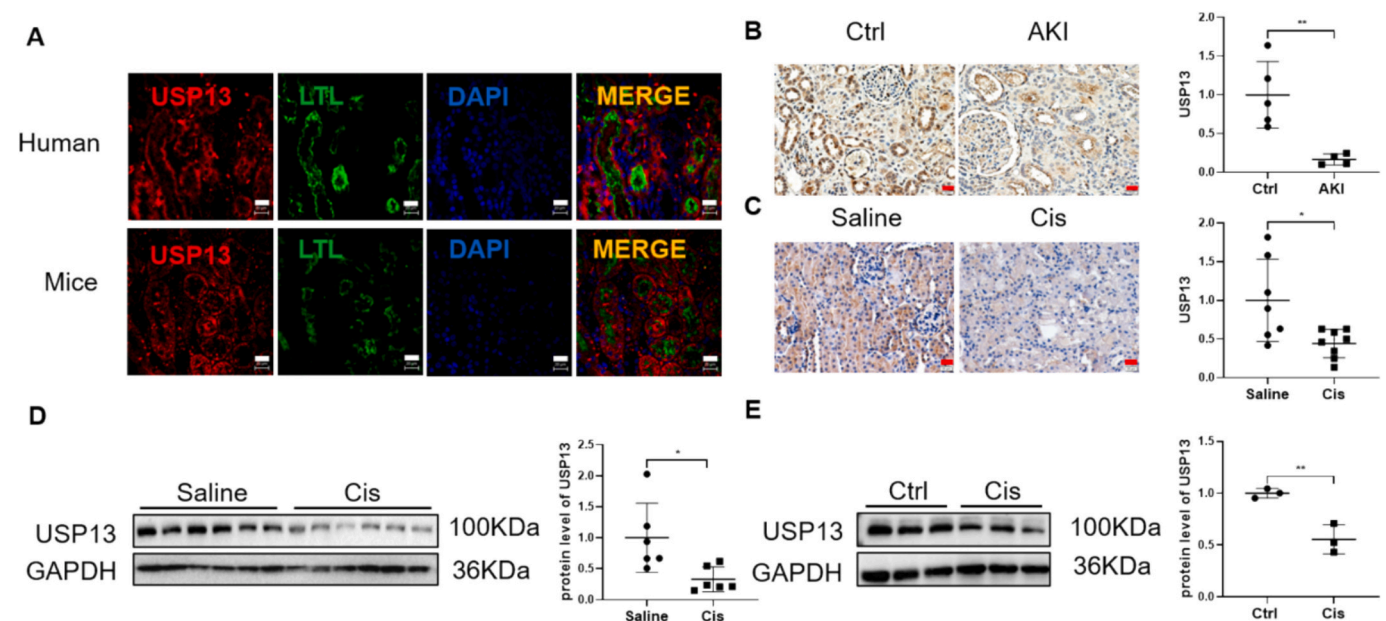


Fig. 1. USP13 is downregulated in AKI. (A) Immunofluorescence co-staining of USP13 with LTL in normal human and mice kidneys, red: USP13, green: LTL, blue: DAPI, scale bars: 20 µm. (B) Immunohistochemical staining of USP13 in the kidney biopsy samples from AKI patients and normal controls, scale bars: 20 µm (*n* = 4–5 in each group). (C) Immunohistochemical staining of USP13 in cisplatin-treated mice kidney tissue, scale bars: 20 µm (*n* = 7 or 8). (D) Western blot analysis of USP13 expression in the kidneys of mice challenged by cisplatin (*n* = 6 in each group). (E) Western blot analysis of USP13 in cisplatin-treated mouse renal epithelial cells (*n* = 3 in each group). Data are expressed as means ± SEM. Student's *t*-test was used to determine the *p*-values. **p* < 0.05, ***p* < 0.01.

higher in Het + Cis mice than that in WT + Cis mice (Fig. 2D, E). Moreover, TUNEL staining suggested that USP13 knockdown promoted cell apoptosis, supported by increased TUNEL-positive cells (Fig. 2F). Additionally, we utilized FA to induce kidney injury in het mice, further validating the role of USP13 in different AKI models. Consistently, Het + FA mice displayed aggravated renal function loss, kidney pathological damage, and tubular injury, compared to WT + FA mice (Fig. S1). These results suggest that loss of USP13 function can accelerate AKI progression.

3.3. Pharmacological inhibition of USP13 exacerbated cisplatin-induced AKI

Based on the effects of USP13 genetic interference on AKI, we used

spautin-1, a reported USP13 inhibitor, to further verify its role in cisplatin-induced AKI. Consistent with the exacerbated renal injury observed in USP13 het mice, spautin-1 treatment further deteriorated renal function, pathological kidney damage, tubular injury, inflammatory response, and cell apoptosis (Fig. 3). Collectively, these results indicated that both genetic loss and pharmacological inhibition of USP13 aggravated cisplatin or FA-induced AKI.

3.4. USP13 overexpression alleviated cisplatin-induced AKI

To better understand the effects of USP13 on cisplatin-induced AKI, we overexpressed USP13 in the kidneys of WT mice using tail vein injection of plasmids (Fig. 4A). A variety of studies, including our preliminary work, have verified the feasibility of this technique [39,40].

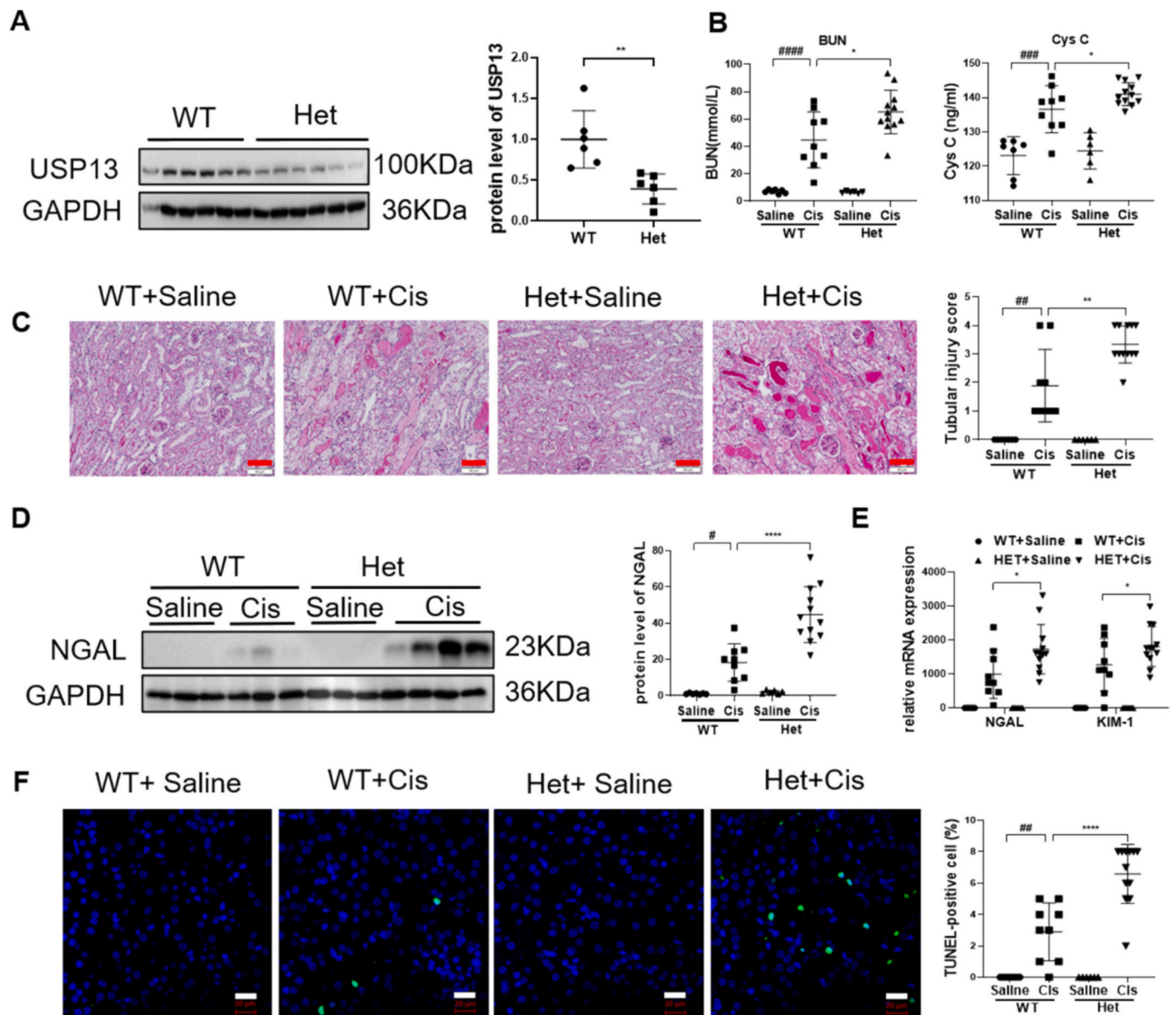


Fig. 2. USP13 knockdown aggravated cisplatin-induced AKI. (A) Western blot analysis of USP13 in the kidneys of WT and Het mice ($n = 6$). (B) Analysis of serum BUN and Cys C in WT and Het mice challenged by cisplatin. (C) Representative images of renal PAS staining in cisplatin-challenged WT and Het mice and analysis of tubular injury score, scale bars: 50 μ m. (D) Western blot analysis of NGAL expression in cisplatin-treated WT and Het mice. (E) RT-qPCR analysis of NGAL and KIM-1 expression in cisplatin-treated WT and Het mice. (F) Representative images of renal TUNEL staining in cisplatin-challenged WT and Het mice and quantification of TUNEL-positive cells, scale bars: 20 μ m. Data are expressed as means \pm SEM ($n = 7$ in WT + Saline group, $n = 9$ in WT + Cis group, $n = 6$ in Het + Saline group, and $n = 12$ in Het + Cis group). Student's t -test and one-way ANOVA were used to determine the p -values. #/ $^{*}p < 0.05$, ##/ $^{**}p < 0.01$, ###/ $^{***}p < 0.001$, ####/ $^{****}p < 0.0001$.

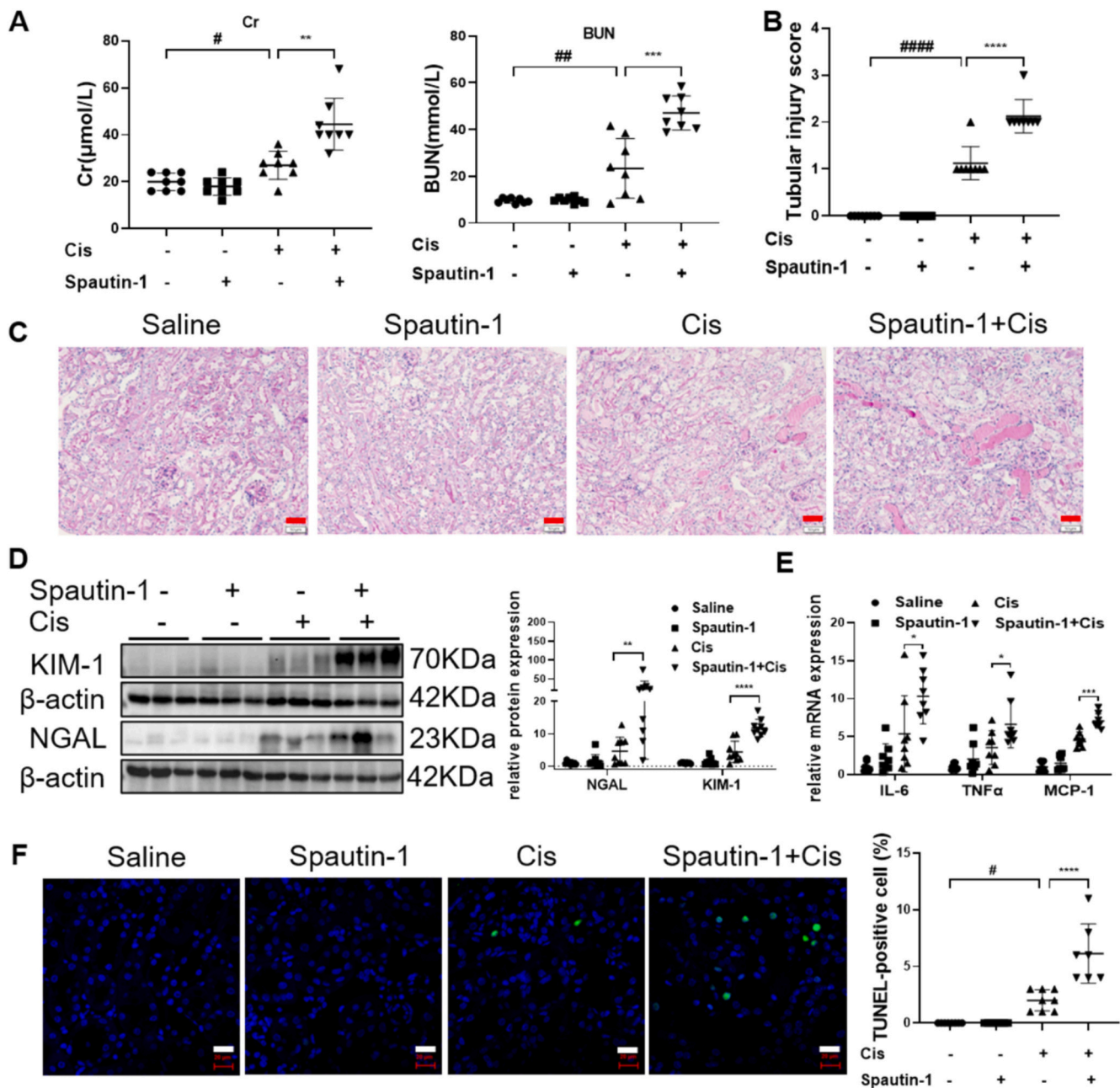


Fig. 3. USP13 inhibition exacerbated cisplatin-induced AKI. (A) Analysis of serum Cr and BUN levels in mice treated with spautin-1 or vehicle, with or without cisplatin treatment. (B, C) Analysis of tubular injury score and representative images of renal PAS staining in cisplatin-challenged mice with or without spautin-1 treatment, scale bars: 50 μm. (D) Western blot analysis of NGAL and KIM-1 expression in cisplatin-challenged mice treated with or without spautin-1 treatment. (E) RT-qPCR analysis of inflammatory factors IL-6, TNFα, and MCP-1 expression in cisplatin-challenged mice with or without spautin-1 treatment. (F) Representative images of renal TUNEL staining in cisplatin-challenged mice with or without spautin-1 treatment, and quantification of TUNEL-positive cells, scale bars: 20 μm. Data are expressed as means ± SEM ($n = 7-9$ in each group). One-way ANOVA was used to determine the p -values. #/ $p < 0.05$, ##/ $p < 0.01$, ****/ $p < 0.001$, #####/ $p < 0.0001$.

These mice were subjected to cisplatin treatment to induce AKI. Compared to mice in the Vector+Cis group, mice in the USP13 + Cis group showed decreased levels of BUN and Cr, indicating that USP13 may protect renal function (Fig. 4B). In agreement with the improvement in renal function of mice in the USP13 + Cis group, USP13 overexpression alleviated pathological kidney damage, tubular injury, inflammation, and cell apoptosis, as evidenced through PAS staining, western blotting, RT-qPCR, and TUNEL staining (Fig. 4C-G). These data suggested that USP13 protected against cisplatin-induced kidney injury.

3.5. USP13 knockdown or overexpression aggravated or attenuated cisplatin-induced renal epithelial cell injury

Considering the damage caused by cisplatin to tubular epithelial cells, we explored the role of USP13 in cisplatin-challenged mPTCs. We first transfected mPTCs with USP13 siRNA to knock down USP13 expression, and then treated the cells with cisplatin (Fig. 5A). CCK8 assay showed that USP13 knockdown markedly decreased cell viability and further exacerbated cisplatin-induced cell death (Fig. 5B). In agreement with the reduced cell viability, flow cytometric analysis verified that cisplatin induced prominent cell death, and USP13

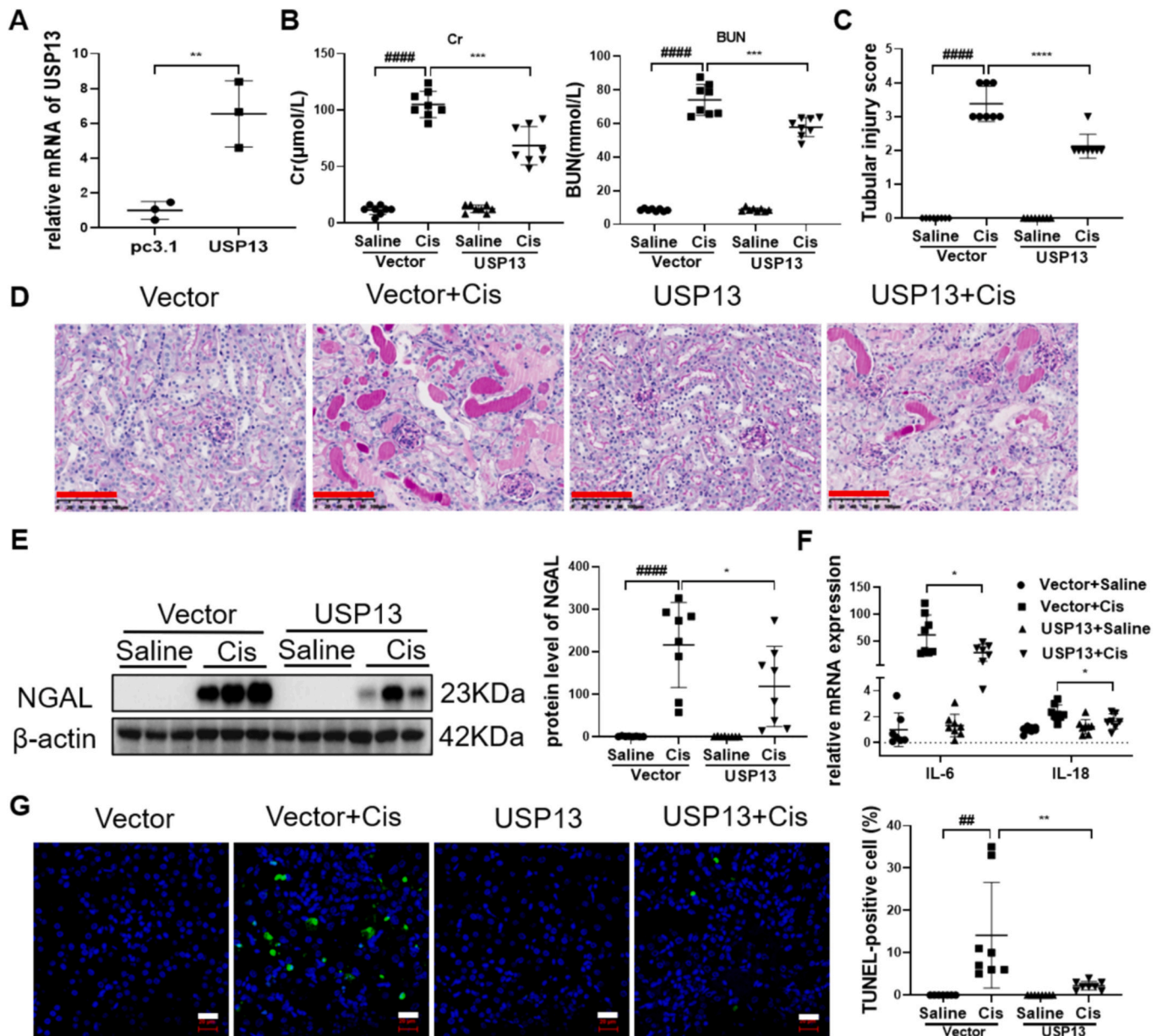


Fig. 4. USP13 overexpression alleviated cisplatin-induced AKI. (A) RT-qPCR analysis of USP13 expression in the kidneys of mice injected with USP13 or scrambled plasmids ($n = 3$ in each group). (B) Analysis of serum Cr and BUN in cisplatin-treated mice with or without USP13 overexpression ($n = 8$ in each group). (C, D) Analysis of tubular injury score and representative images of renal PAS staining in cisplatin-challenged mice with or without USP13 overexpression, scale bars: 100 μm ($n = 8$ in each group). (E) Western blot analysis of tubular injury marker NGAL expression in cisplatin-treated mice with or without USP13 overexpression ($n = 8$ in each group). (F) RT-qPCR analysis of inflammatory factors IL-6 and IL-18 in cisplatin-treated mice with or without USP13 overexpression ($n = 7$ or 8 in each group). (G) Representative images of renal TUNEL staining in cisplatin-challenged mice and quantification of TUNEL-positive cells, scale bars: 20 μm ($n = 7$ or 8 in each group). Data are expressed as means \pm SEM. Student's t -test and one-way ANOVA were used to determine the p -values. $^{*}p < 0.05$, $^{**}p < 0.01$, $^{***}p < 0.001$, $^{####}p < 0.0001$.

knockdown led to increased cell death (Fig. 5C, D). USP13 knockdown alone induced significant cell death in vitro, indicating that USP13 may greatly affected cell survival and death pathways via unknown mechanisms. However, this phenomenon was not observed in the kidney tissues of *Usp13* het mice, possibly owing to cellular crosstalk in vivo, which may prevent USP13 function loss-induced cell death. Additionally, western blotting confirmed increased apoptosis in mPTCs transfected with USP13 siRNA, as shown by the reduced expression of BCL-2, a well-known apoptotic marker in injured kidneys [41,42] (Fig. 5E). Furthermore, RT-qPCR results showed that USP13 knockdown further promoted the upregulation of the tubule injury marker NGAL and pro-inflammatory factors IL-6, TNF α , and MCP-1 (Fig. 5F).

Simultaneously, HK-2 cells were also used to assess the function of USP13. Consistently, USP13 knockdown further aggravated cisplatin-induced cell death and inflammation in HK2 cells (Fig. S2).

Based on the detrimental effects of USP13 downregulation on cisplatin-induced AKI, we explored whether USP13 overexpression could provide renal protection. Similarly, mPTCs were transfected with USP13 plasmids, and western blotting confirmed the successful overexpression of USP13 (Fig. 5G). CCK8, flow cytometry, western blotting, and RT-qPCR results showed that USP13 overexpression markedly restored cell viability, inhibited cell death, and mitigated the inflammatory response in mPTCs challenged by cisplatin (Fig. 5H-L). These data indicated that USP13 upregulation could protect against cisplatin-

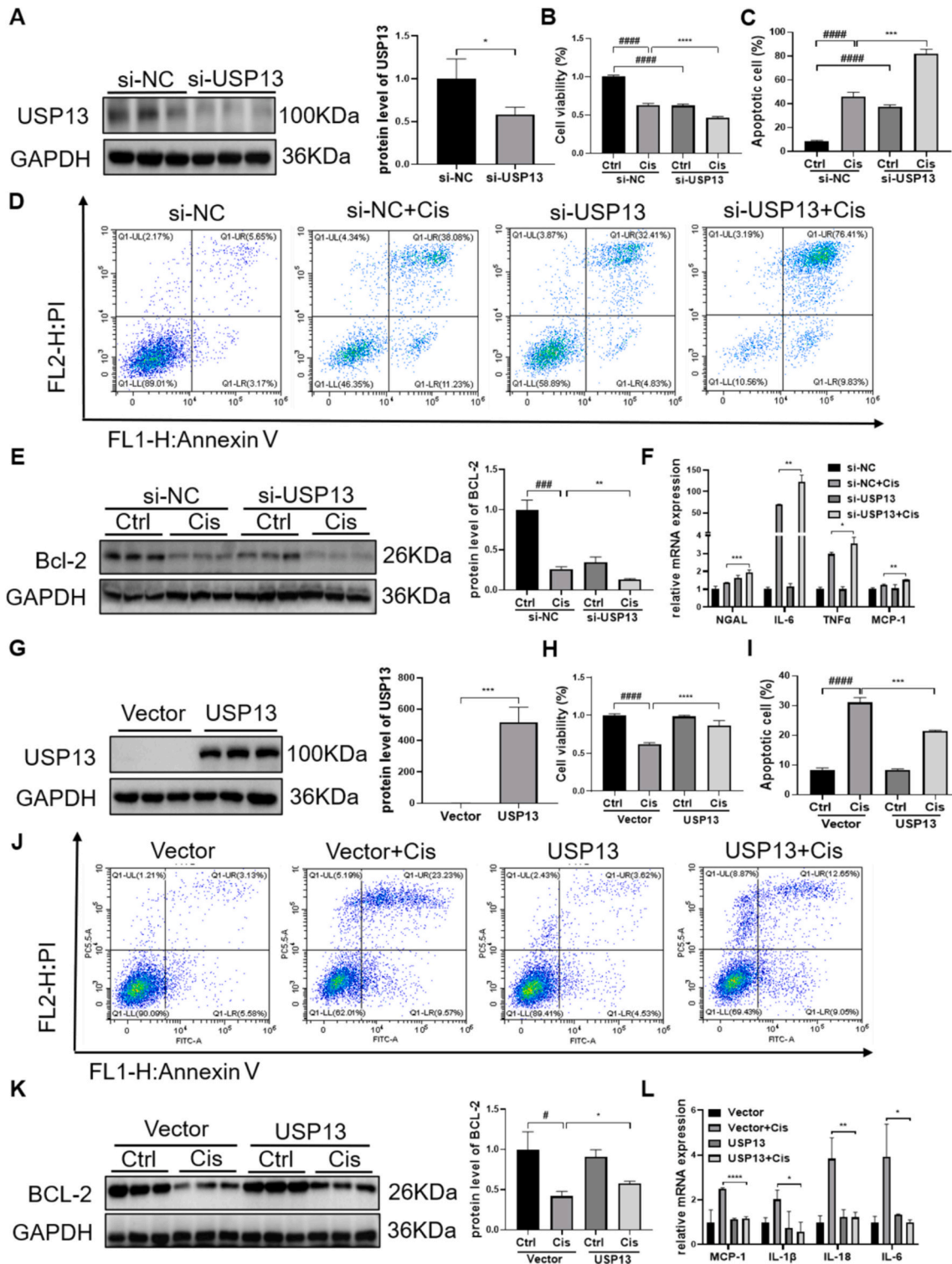


Fig. 5. USP13 knockdown or overexpression aggravated or attenuated cisplatin-induced renal epithelial cell injury. (A) Western blot analysis of USP13 expression in mPTCs transfected with USP13 siRNA or negative control (NC). (B) CCK8 assay for cell viability in cisplatin-induced mPTCs transfected with USP13 siRNA or NC. (C, D) Flow cytometric analysis for cell apoptosis in cisplatin-induced mPTCs transfected with USP13 siRNA or NC. (E) Western blot analysis of BCL-2 expression in cisplatin-induced mPTCs transfected with USP13 siRNA or NC. (F) RT-qPCR analysis of NGAL and pro-inflammatory factors (IL-6, TNF α , and MCP-1) in cisplatin-induced mPTCs transfected with USP13 siRNA or NC. (G) Western blot analysis of USP13 expression in mPTCs transfected with USP13 or scrambled plasmids. (H) CCK8 assay for cell viability in cisplatin-induced mPTCs transfected with USP13 or scrambled plasmids. (I, J) Flow cytometric analysis for cell apoptosis in cisplatin-induced mPTCs transfected with USP13 or scrambled plasmids. (K) Western blot analysis of BCL-2 expression in cisplatin-induced mPTCs transfected with USP13 or scrambled plasmids. (L) RT-qPCR analysis of pro-inflammatory factors MCP-1, IL-1 β , IL-18, and IL-6 in cisplatin-induced mPTCs transfected with USP13 or scrambled plasmids. Data are expressed as means \pm SEM ($n = 3$ in each group). Student's t -test and one-way ANOVA were utilized to determine the p -values. #/ $p < 0.05$, **/ $p < 0.01$, ###/ $p < 0.001$, ####/ $p < 0.0001$.

induced renal injury by inhibiting cell death and attenuating inflammation, whereas USP13 downregulation advanced the progression of cell injury.

3.6. MCL-1 was a deubiquitinating substrate of USP13 and reduced MCL-1 aggravated mitochondrial dysfunction in cisplatin-induced AKI

MCL-1 has been identified as a USP13 substrate [16]. Based on the anti-apoptotic role and mitochondrial regulation of MCL-1, we hypothesized that USP13 may target MCL-1 to regulate mitochondrial function in cisplatin-induced kidney injury. Immunofluorescence revealed the mitochondrial localization of USP13 and its colocalization with MCL-1. This was supported by the colocalization of USP13 with the mitochondrial outer membrane protein TOM20 and MCL-1 in mPTCs (Fig. 6A). To observe the interaction between USP13 and MCL-1, we conducted molecular docking and computer simulations. The predicted binding sites in humans and mice are shown in Fig. 6B (Fig. 6B). Co-immunoprecipitation further validated USP13-MCL-1 interaction in mPTCs and 293T cells (Fig. 6C and Fig. S3A). In addition, western blotting showed that USP13 knockdown or overexpression decreased or increased MCL-1 protein levels, respectively, in vitro and in vivo,

indicating the regulation of USP13 on MCL-1 expression (Fig. 6D and Fig. S3B, C). As a DUB, USP13 protects its substrates from proteasomal degradation. Therefore, the proteasome inhibitor, MG132, was used to evaluate the effect of USP13 on MCL-1 stability. As previous studies have indicated that MG132 could affect the expression of cytosolic proteins including GAPDH and β -actin, we used nuclear membrane protein LaminB1 as an internal control here [43,44]. As shown in Fig. 6E, the knockdown or inhibition of USP13 induced a significant decline in MCL-1 protein levels, whereas proteasome suppression by MG132 significantly restored MCL-1 expression, indicating that USP13 loss leads to increased MCL-1 degradation via the proteasomal pathway (Fig. 6E). Furthermore, an in vivo MCL-1 ubiquitination assay revealed that USP13 reduced the levels of ubiquitinated MCL-1 (Fig. 6F). These data demonstrate that MCL-1 is a deubiquitinating substrate of USP13.

MCL-1 has been documented to regulate cell apoptosis and mitochondrial function [28]. Therefore, we explored the function of MCL-1 in cell death and mitochondrial function in cisplatin-treated mPTCs. We first transfected mPTCs with MCL-1 siRNA and performed western blotting and RT-qPCR to confirm the successful knockdown of MCL-1 (Fig. S3D, E). Flow cytometry showed that MCL-1 knockdown significantly induced and aggravated cisplatin-induced cell death (Fig. S3F).

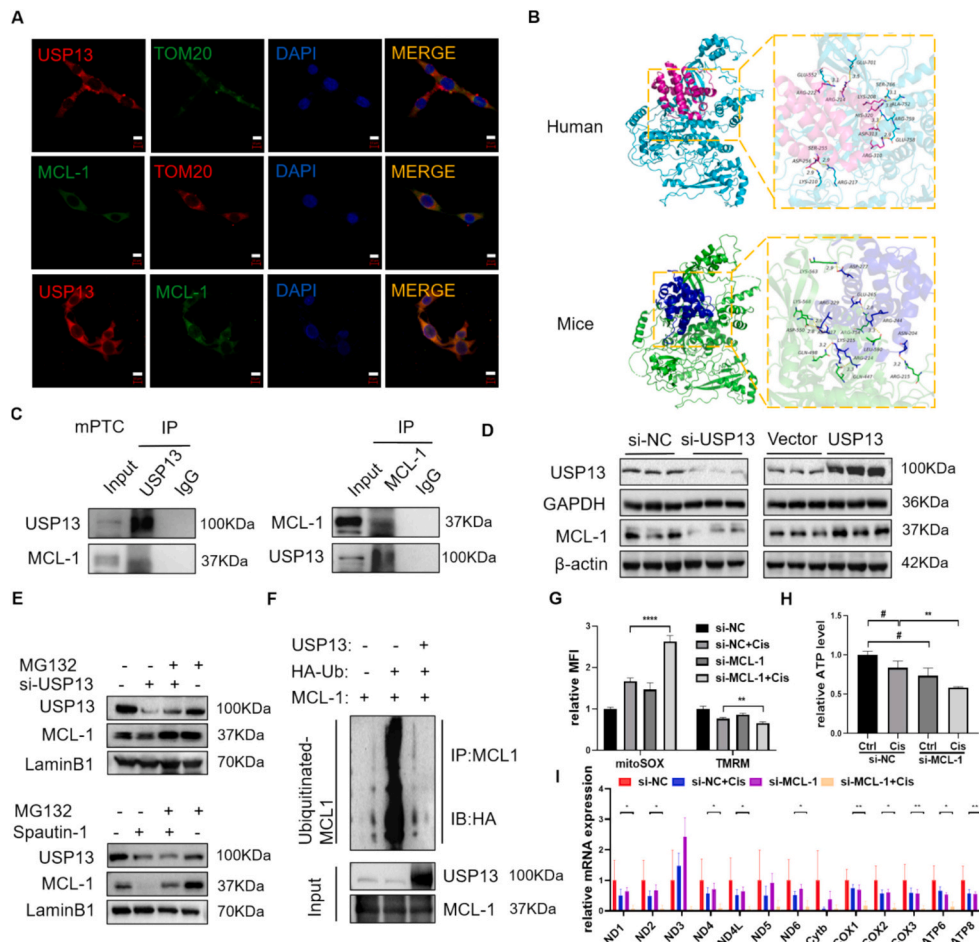


Fig. 6. MCL-1 was a deubiquitinating substrate of USP13 and reduced MCL-1 aggravated mitochondrial dysfunction in cisplatin-induced renal tubular epithelial cell injury. (A) Immunofluorescence co-staining of USP13 with TOM20, MCL-1 with TOM20, USP13 with MCL-1 in mPTCs, scale bars: 20 μ m. (B) The binding modes of the complex USP13 with MCL-1 in humans and mice, humans: USP13 was colored in cyan and MCL-1 was colored red, mice: USP13 was colored in green and MCL-1 was colored blue. (C) Co-IP analysis of the interaction between USP13 and MCL-1 in mPTCs. (D) Western blot analysis of MCL-1 expression in mPTCs transfected with USP13 si-RNA or plasmids. (E) Western blot analysis of MCL-1 expression in mPTCs with proteasome inhibitor MG132 treatment after USP13 knockdown or inhibition. (F) In vivo ubiquitination assay for the ubiquitinated level of MCL-1 in 293T cells. (G) Flow cytometric analysis of mitoROS or MMP in cisplatin-induced mPTCs with or without MCL-1 knockdown. (H) Luciferase assay for cellular ATP content in cisplatin-induced mPTCs with or without MCL-1 knockdown. (I) RT-qPCR analysis of mitochondrial respiratory chain genes in cisplatin-treated mPTCs with or without MCL-1 knockdown. Data are presented as means \pm SEM ($n = 3$ in each group). Student's t -test and one-way ANOVA were used to determine the p -values. #/ $^*p < 0.05$, $^{**}p < 0.01$, $^{***}p < 0.0001$.

Considering the essential role of MCL-1 in the mitochondria, we next explore how MCL-1 influences mitochondrial function in cisplatin-treated renal epithelial cells. As shown in Fig. 6G and H, cisplatin treatment resulted in increased mitoROS, decreased MMP, and reduced ATP content, which were further exacerbated by MCL-1 knockdown (Fig. 6G, H). A previous study indicated that MCL-1 deletion could decrease the expression of mtDNA-encoded COX1 and COX2, which may be explained by a reduction of mtDNA [28]. Consistently, our RT-qPCR results revealed that downregulation of MCL-1 facilitated the decline of mitochondrial respiratory chain-related genes in cisplatin-stimulated

mPTCs (Fig. 6I). Furthermore, the lack of MCL-1 also disrupted mitochondrial dynamics, represented by the marked downregulation of mitochondrial fusion proteins including OPA1 and mitofusin 1/2 (MFN1/2), as well as fission proteins including DRP1, mitochondrial fission factor (MFF), and fission, mitochondrial 1 (FIS1), at the protein and mRNA levels (Fig. S3G, H). These data indicated that MCL-1 reduction resulting from USP13 downregulation accelerated cisplatin-induced renal tubular cell injury by promoting cell death and mitochondrial dysfunction.

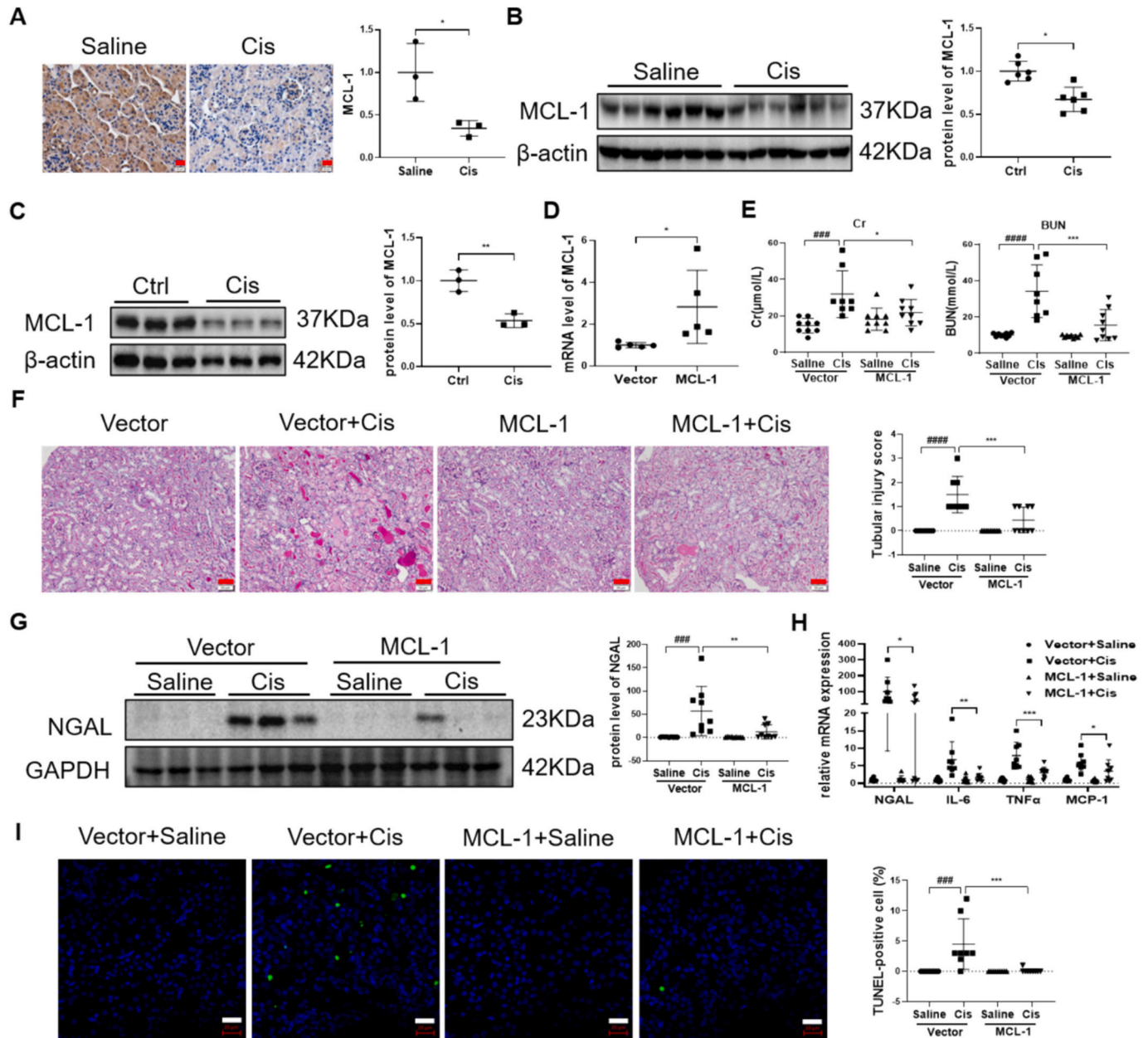


Fig. 7. MCL-1 overexpression ameliorates cisplatin-induced AKI. (A) Immunohistochemical staining of MCL-1 in cisplatin-treated mice kidney tissues, scale bars: 20 μ m. (B) Western blot analysis of MCL-1 expression in the kidneys of cisplatin-challenged mice ($n = 6$ in each group). (C) Western blot analysis of MCL-1 in cisplatin-treated mouse renal epithelial cells ($n = 3$ in each group). (D) RT-qPCR analysis of MCL-1 expression in the kidneys of mice injected with scrambled or MCL-1 plasmids ($n = 5$). (E) Measurements of serum Cr and BUN in cisplatin-induced mice with or without MCL-1 overexpression. (F) Representative images of renal PAS staining in cisplatin-induced mice injected with MCL-1 or scrambled plasmids and analysis of tubular injury score, scale bars: 50 μ m. (G) Western blot analysis of tubular injury marker NGAL expression in cisplatin-induced mice injected with MCL-1 or scrambled plasmids. (H) RT-qPCR analysis of NGAL and inflammatory factors (IL-6, TNF α , and MCP-1) in cisplatin-induced mice with or without MCL-1 overexpression. (I) Representative images of renal TUNEL staining in cisplatin-induced mice injected with MCL-1 or scrambled plasmids and quantification of TUNEL-positive cells, scale bars: 20 μ m. Data are expressed as means \pm SEM ($n = 8-9$ in each group). Student's t -test and one-way ANOVA were used to determine the p -values. * $p < 0.05$, ** $p < 0.01$, *** $p < 0.001$, **** $p < 0.0001$.

3.7. MCL-1 overexpression ameliorated cisplatin-induced AKI

Next, we examine whether MCL-1 protects against renal damage in cisplatin-challenged mice. In agreement with USP13 reduction in AKI, MCL-1 was significantly downregulated in cisplatin-treated mouse kidneys and mPTCs, as evidenced via IHC and western blotting (Fig. 7A-C). Similarly, we overexpressed MCL-1 via tail vein injection of MCL-1 plasmids, and RT-qPCR analysis confirmed the high expression of MCL-1 in the kidneys (Fig. 7D). Consistent with the results in mice overexpressing USP13, high MCL-1 expression significantly ameliorated cisplatin-induced renal function decline, pathological kidney damage, tubular injury, renal inflammation, and apoptosis (Fig. 7E-I). Summarily, in cisplatin-induced AKI, MCL-1 functioned as a downstream substrate of USP13 and exerted renoprotective effects.

3.8. USP13 knockdown deteriorated mitochondrial function in cisplatin-treated mPTCs

Given the regulation of MCL-1 in mitochondrial function, we examined whether USP13, an upstream modulator of MCL-1, displayed similar effects. Consistent with the results in cells transfected with MCL-1 siRNA, USP13 knockdown exacerbated mitochondrial dysfunction. As shown in Fig. 8A and B, USP13 knockdown further aggravated cisplatin-induced ATP reduction, MMP decrease, and ROS overproduction (Fig. 8A, B). Additionally, USP13 knockdown markedly inhibited the expression of mitochondrial respiratory chain-associated genes, and reduced the capacity for mitochondrial respiration (Fig. 8C-E). Moreover, knockdown of USP13 also disturbed mitochondrial dynamics, as shown by the downregulated expression of mitochondrial fusion- and fission- related genes (Fig. 8F, G). Taken together, these findings

suggested that USP13 loss impaired mitochondrial function and exacerbated cisplatin-induced tubular epithelial cell injury.

4. Discussion

Owing to their high energy demand, renal tubular epithelial cells are particularly susceptible to various stimuli, making them prone to injury. Therefore, exploring novel targets to protect the renal tubular epithelial cells from injury may prevent or delay AKI progression. In the present study, we explored the role and potential mechanism of USP13 in AKI. USP13 knockdown or inhibition accelerated kidney damage by aggravating MCL-1 reduction-mediated mitochondrial dysfunction and cell death, whereas USP13 overexpression attenuated kidney injury.

Protein ubiquitination and deubiquitination are involved in various pathologies including AKI. Mounting evidence has shown that several DUBs (USP25 [45], USP14 [46], and USP7 [47]) have detrimental effects on kidney injury, whereas USP36 [48] and USP10 [49] show renal protection. Based on the controversial roles of these USPs in AKI, we discussed how USP13, another member of the USPs family, acted in AKI. Increasing evidence has revealed a role for USP13 in inflammation, oxidative stress, and apoptosis, all of which contributes to the development of renal injury. In arthritic mice and cell models, USP13 overexpression significantly inhibited inflammation, ROS generation, and cell apoptosis [50]. Additionally, single immunoglobulin interleukin-1 (IL-1)-related receptor (Sigirr), an anti-inflammatory receptor, has been considered as a USP13 substrate [51]. Under LPS stimulation, USP13 expression was significantly reduced and mice deficient of *Usp13* exhibited increased inflammatory cell infiltration, which was partly reversed by Sigirr overexpression [51,52]. Consistently, myeloid-specific deficiency of *Usp13* promoted LPS-induced expression and

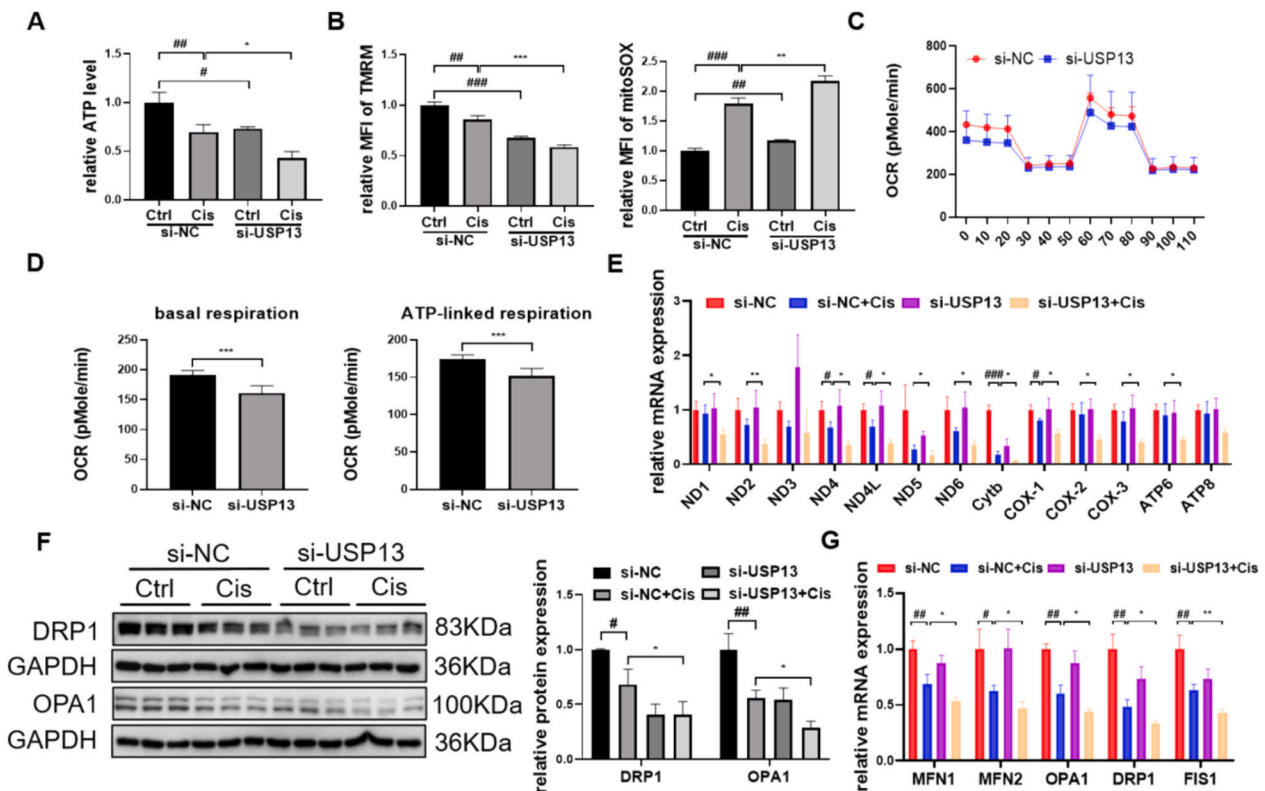


Fig. 8. USP13 knockdown deteriorated mitochondrial function in cisplatin-treated mPTCs. (A) Luciferase assay for cellular ATP content in cisplatin-induced mPTCs with or without USP13 knockdown. (B) Flow cytometric analysis for MMP or mitoROS of cisplatin-induced mPTCs with or without USP13 knockdown. (C, D) Seahorse analysis for oxygen consumption rate of mPTCs transfected with USP13 siRNA or NC ($n = 5$ or 6). (E) RT-qPCR analysis of mitochondrial respiratory chain genes in cisplatin-induced mPTCs with or without USP13 knockdown. (F) Western blot analysis of DRP1 and OPA1 in cisplatin-induced mPTCs with or without USP13 knockdown. (G) RT-qPCR analysis of MFN1/2, OPA1, DPR1, MFF, and FIS1 in mPTCs transfected with USP13 siRNA or NC. Data are expressed as means \pm SEM ($n = 3$ in each group). Student's t-test and one-way ANOVA were used to determine the p-values. #/ $p < 0.05$, ##/ $p < 0.01$, ###/ $p < 0.001$, ####/ $p < 0.0001$.

excretion of inflammatory factors [53]. In line with these investigations, our data indicated that USP13 overexpression inhibited the expression of pro-inflammatory factors and cell apoptosis to attenuate cisplatin-induced AKI, whereas knockdown or inhibition of USP13 displayed the opposite effects. However, some studies have shown that USP13 promotes inflammation. In response to extracellular ATP, paxillin functions as an adaptor factor, bridging the plasma membrane channel P2X7 receptor and the NLRP3 inflammasome to facilitate NLRP3 inflammasome activation, during which USP13 serves as a helper in paxillin-mediated NLRP3 deubiquitination [54]. Moreover, in contrast to the reduction of USP13 in LPS-treated lungs, USP13 is upregulated in the brains of rats subjected to ischemia-reperfusion injury. Pretreatment with the USP13 inhibitor spautin-1 attenuates cerebral IR injury by reducing NLRP3, the autophagy-related protein Beclin1, and the pyroptosis executor GSDMD-N expression [55]. Considering the diversity of inflammatory signaling pathways, USP13 may play opposing roles in different pathological states.

MCL-1 is a member of the BCL-2 family, and its anti-apoptotic properties play important roles in many kinds of diseases. Research has demonstrated that MCL-1 could antagonize apoptosis or induce mitophagy to protect neuronal cells in Alzheimer's and Parkinson's disease models [56–58]. In addition, MCL-1 ameliorated liver injury and fibrosis in bile duct-ligated mice, which was attributed to its anti-apoptotic role [59]. In terms of kidney injury, MCL-1 was observed downregulated in cisplatin and indomethacin-treated renal epithelial cells, and MCL-1 rescue by proteasome inhibitors could promote cell survival [60–62]. Consistent with these previous studies, we observed a significant reduction in MCL-1 expression in cisplatin-treated mouse kidneys and renal epithelial cells. As no in vivo studies have described the detailed function of MCL-1 in injured kidneys, we overexpressed MCL-1 in the kidneys of mice to examine whether MCL-1 protected against kidney injury. The results showed that MCL-1 overexpression markedly restored renal function, mitigated renal tubular injury, prevented the upregulation of inflammatory factors, and suppressed apoptosis. However, in a previous study, MCL-1 overexpression in hematopoietic cells did not display protective effects but accelerated the onset of lymphadenopathy, splenomegaly, and autoimmune diseases in *Fas^{lpr/lpr}* mice by increasing lymphoid populations [63]. This suggests that the anti-apoptotic role of MCL-1 may be beneficial or detrimental under different conditions. Additionally, it was recently reported that USP13 deubiquitinated and stabilized MCL-1 to promote tumor cell survival in several tumor types [11,16]. In the present study, USP13-mediated MCL-1 stabilization in renal tubular epithelial cells protected against renal injury.

In addition to inhibiting apoptosis, MCL-1 is also indispensable for maintaining normal mitochondrial structure and function. MCL-1 has two mitochondrial sub-localizations: the outer mitochondrial membrane isoform (MCL-1^{OMM}) functions like other BCL-2 anti-apoptotic factors, while the mitochondrial matrix isoform (MCL-1^{matrix}) is essential for normal inner mitochondrial membrane structure, oxidative phosphorylation, assembly of F1F0-ATP synthase oligomers, and mitochondrial fusion and fission [28]. In the present study, MCL-1 loss not only induced renal epithelial cell apoptosis but also impaired mitochondrial respiration, and ATP generation, and disturbed mitochondrial dynamics, confirming the irreplaceable role of MCL-1 in mitochondrial homeostasis. Mitochondrial dysfunction is a key mechanism that contributes to AKI progression. Mounting evidence has demonstrated mitochondrial structural damage accompanied by functional loss including MMP decrease, ROS generation, mtDNA loss, ATP exhaustion, as well as impaired respiratory function in injured kidneys [34,64,65]. Our study supported these findings and revealed that USP13 knockdown aggravated the loss of mitochondrial function. Mitochondria are organelles that maintain a dynamic balance via fusion and fission. Mitochondrial fusion is primarily mediated by MFN1/2 and OPA1, whereas mitochondrial fission is primarily dependent on DRP1 and FIS1 [66]. In cisplatin-, IR injury-, and cecal ligation and puncture-induced kidneys,

DRP1 is reportedly upregulated, while OPA1 is downregulated, leading to mitochondrial fragmentation; conversely, knockdown or inhibition of DRP1 ameliorates mitochondrial dysfunction by depressing mitochondrial fission [67,68]. However, in our study, after cisplatin treatment, both DRP1 and OPA1 levels in mPTCs were markedly reduced, which may be the result of excessive mitochondrial loss. In addition, disruption of mitochondrial dynamics was observed in mPTCs transfected with USP13 and MCL-1 siRNAs. These results suggested that USP13 regulated mitochondrial function via MCL-1.

A limitation of our study is that as a deubiquitinating enzyme, USP13 may target other substrates in AKI, which requires further exploration. Many studies have revealed the role of USP13 in autophagy. Based on the importance of autophagy in AKI, autophagy-related substrates such as Beclin1, ATG5, and p62 may serve as downstream of USP13 in AKI, which needs to be explored [69–71]. Additionally, metabolic disorder is also associated with AKI development; under this circumstance, USP13 may regulate lipid metabolism via FASN during AKI progression [72]. In addition to these known reported substrates, predication of protein-protein interactions and molecular docking may reveal novel USP13 substrates. Another limitation is that the mechanism by which USP13 expression is reduced has not yet been elucidated. Recent studies have described some factors that regulate USP13 activity, such as Beclin1 [69], RAP80 [73], casein kinase 2 [74], and miR-135b [75], some of which may serve as upstream modulators of USP13 in AKI.

In summary, our study demonstrated that under cisplatin challenge, USP13 downregulation in renal epithelial cells failed to stabilize MCL-1, thereby resulting in MCL-1 reduction and consequent mitochondrial dysfunction and cell death, accelerating AKI progression. The findings of this study not only enhance our knowledge of the AKI pathogenesis but also broaden the spectrum of USP13 in diseases. Overall, these findings suggest that USP13 is a potential therapeutic target for AKI prevention and treatment.

Supplementary data to this article can be found online at <https://doi.org/10.1016/j.bbadis.2024.167599>.

Abbreviations

AKI	Acute kidney injury
BUN	Serum blood urea nitrogen
CCK8	Cell counting kit 8
Cys C	Cystatin C
DRP1	Dynamin-related protein 1
DUB	Deubiquitinase
FIS1	Fission mitochondrial 1
Het	Heterozygote
IF	Immunofluorescence
IL-1/6/18	Interleukin-1/6/18
IHC	Immunohistochemistry
IP	Immunoprecipitation
KIM-1	Kidney injury molecule 1
KO	Knockout
LPS	Lipopolysaccharide
LTL	Lotus tetragonolobus lectin
MCL-1	Myeloid cell leukemia 1
MF1	Mitochondrial fission factor
MFN1/2	Mitofusin 1/2
mitoROS	mitochondrial Reactive oxygen species
MMP	Mitochondrial membrane potential
mPTC	Mouse proximal tubule epithelial cell
NGAL	Neutrophil gelatinase-associated lipocalin
NC	Negative control
OCR	Oxygen consumption rate
OPA1	Optic atrophy protein 1
PAS	Periodic acid-schiff
TNF- α	Tumor necrosis factor
TOM20	Translocase of outer mitochondrial membrane 20

TUNEL TdT mediated dUTP nick end labeling
 USP13 Ubiquitin-specific protease 13
 WT Wild-type

CRedit authorship contribution statement

Qian Wang: Writing – review & editing, Writing – original draft, Visualization, Validation, Methodology, Investigation, Formal analysis, Data curation, Conceptualization. **Shihan Cao:** Writing – review & editing, Methodology, Investigation, Conceptualization. **Zhenzhen Sun:** Writing – review & editing, Investigation, Formal analysis. **Wenping Zhu:** Writing – review & editing, Investigation, Data curation. **Le Sun:** Writing – review & editing, Methodology, Conceptualization. **Yuanyuan Li:** Writing – review & editing, Funding acquisition, Data curation. **Dan Luo:** Writing – review & editing, Methodology. **Songming Huang:** Writing – review & editing, Supervision, Conceptualization. **Yue Zhang:** Writing – review & editing, Supervision, Conceptualization. **Weiwei Xia:** Writing – review & editing, Supervision, Project administration, Funding acquisition, Conceptualization. **Aihua Zhang:** Writing – review & editing, Supervision, Project administration, Funding acquisition, Conceptualization. **Zhanjun Jia:** Writing – review & editing, Supervision, Project administration, Funding acquisition, Conceptualization.

Consent for publication

All authors agree to the publication of this study.

Ethical approval and consent to participate

The clinical study got approval from the Ethics Committee of Children's Hospital of Nanjing Medical University (202404030-1). All participants have informed consent. The animal experiments were conducted based on the Guide for the Care and Use of Laboratory Animals and got approval from the Animal Care and Use Committee of Nanjing Medical University (2407058).

Funding

This work got grants support from National Key Research and Development Program (2022YFC2705100), National Natural Science Foundations of China (82070701, 82070760, 82100712), Social Development Fund of Jiangsu Province (BE2021607), “333” talent plan of Jiangsu province (333-2022001), and Jiangsu Key discipline of nephrology (ZDXK202204).

Declaration of competing interest

The authors declare that they have no known competing financial interests or personal relationships that could have appeared to influence the work reported in this paper.

Data availability

All data supporting the findings of this study are available from the corresponding author upon reasonable request.

References

- [1] N.H. Lameire, A. Levin, J.A. Kellum, M. Cheung, M. Jadoul, W.C. Winkelmayer, et al., Harmonizing acute and chronic kidney disease definition and classification: report of a Kidney Disease: Improving Global Outcomes (KDIGO) Consensus Conference, *Kidney Int.* 100 (3) (2021) 516–526.
- [2] J. Gameiro, J.A. Fonseca, C. Outerelo, J.A. Lopes, Acute kidney injury: from diagnosis to prevention and treatment strategies, *J. Clin. Med.* 9 (6) (2020).
- [3] S. Peerapornratana, C.L. Manrique-Caballero, H. Gomez, J.A. Kellum, Acute kidney injury from sepsis: current concepts, epidemiology, pathophysiology, prevention and treatment, *Kidney Int.* 96 (5) (2019) 1083–1099.
- [4] P.A. McCullough, J.P. Choi, G.A. Feghali, J.M. Schussler, R.M. Stoler, R. C. Vallabahn, et al., Contrast-induced acute kidney injury, *J. Am. Coll. Cardiol.* 68 (13) (2016) 1465–1473.
- [5] S. Gaudry, P.M. Palevsky, D. Dreyfuss, Extracorporeal kidney-replacement therapy for acute kidney injury, *N. Engl. J. Med.* 386 (10) (2022) 964–975.
- [6] X. Li, G. Yang, W. Zhang, B. Qin, Z. Ye, H. Shi, et al., USP13: multiple functions and target inhibition, *Front. Cell Dev. Biol.* 10 (2022) 875124.
- [7] Q. Wang, Z. Sun, W. Xia, L. Sun, Y. Du, Y. Zhang, et al., Role of USP13 in physiology and diseases, *Front. Mol. Biosci.* 9 (2022) 977122.
- [8] H. Goto, Y. Yasui, A. Kawajiri, E.A. Nigg, Y. Terada, M. Tatsuka, et al., Aurora-B regulates the cleavage furrow-specific vimentin phosphorylation in the cytokinetic process, *J. Biol. Chem.* 278 (10) (2003) 8526–8530.
- [9] Y. Li, K. Luo, Y. Yin, C. Wu, M. Deng, L. Li, et al., USP13 regulates the RAP80-BRCA1 complex dependent DNA damage response, *Nat. Commun.* 8 (2017) 15752.
- [10] X. Liu, M.L. Hebron, S. Mulki, C. Wang, E. Lekah, D. Ferrante, et al., Ubiquitin specific protease 13 regulates tau accumulation and clearance in models of Alzheimer's disease, *J. Alzheimers Dis.* 72 (2) (2019) 425–441.
- [11] E.L. Morgan, M.R. Patterson, D. Barba-Moreno, J.A. Scarth, A. Wilson, A. Macdonald, The deubiquitinase (DUB) USP13 promotes Mcl-1 stabilisation in cervical cancer, *Oncogene* 40 (11) (2021) 2112–2129.
- [12] Y. Wu, Y. Zhang, C. Liu, Y. Zhang, D. Wang, S. Wang, et al., Amplification of USP13 drives non-small cell lung cancer progression mediated by AKT/MAPK signaling, *Biomed. Pharmacother.* 114 (2019) 108831.
- [13] Z. Qu, R. Zhang, M. Su, W. Liu, USP13 serves as a tumor suppressor via the PTEN/AKT pathway in oral squamous cell carcinoma, *Cancer Manag. Res.* 11 (2019) 9175–9183.
- [14] H. Xie, J. Zhou, X. Liu, Y. Xu, A.J. Heppner, J.M. Simon, et al., USP13 promotes deubiquitination of ZHX2 and tumorigenesis in kidney cancer, *Proc. Natl. Acad. Sci. USA* 119 (36) (2022) e2119854119.
- [15] H. Yan, X. Huang, J. Xu, Y. Zhang, J. Chen, Z. Xu, et al., Chloroquine intervenes nephrotoxicity of Nilotinib through deubiquitinase USP13-mediated stabilization of Bcl-XL, *Adv Sci (Weinh.)* 10 (26) (2023) e2302002.
- [16] S. Zhang, M. Zhang, Y. Jing, X. Yin, P. Ma, Z. Zhang, et al., Deubiquitinase USP13 dictates MCL1 stability and sensitivity to BH3 mimetic inhibitors, *Nat. Commun.* 9 (1) (2018) 215.
- [17] R.W. Craig, The bcl-2 gene family, *Semin. Cancer Biol.* 6 (1) (1995) 35–43.
- [18] H. Wang, M. Guo, H. Wei, Y. Chen, Targeting MCL-1 in cancer: current status and perspectives, *J. Hematol. Oncol.* 14 (1) (2021) 67.
- [19] P. Mittal, S. Singh, R. Sinha, A. Shrivastava, A. Singh, I.K. Singh, Myeloid cell leukemia 1 (MCL-1): structural characteristics and application in cancer therapy, *Int. J. Biol. Macromol.* 187 (2021) 999–1018.
- [20] M.E. Turnis, E. Kaminska, K.H. Smith, B.J. Kartchner, P. Vogel, J.D. Laxton, et al., Requirement for antiapoptotic MCL-1 during early erythropoiesis, *Blood* 137 (14) (2021) 1945–1958.
- [21] V. Peperzak, I. Vikstrom, J. Walker, S.P. Glaser, M. LePage, C.M. Coquery, et al., Mcl-1 is essential for the survival of plasma cells, *Nat. Immunol.* 14 (3) (2013) 290–297.
- [22] H. Hikita, T. Takehara, S. Shimizu, T. Kodama, W. Li, T. Miyagi, et al., Mcl-1 and Bcl-xL cooperatively maintain integrity of hepatocytes in developing and adult murine liver, *Hepatology* 50 (4) (2009) 1217–1226.
- [23] A. Dunkle, I. Dzhalalov, Y.W. He, Mcl-1 promotes survival of thymocytes by inhibition of Bak in a pathway separate from Bcl-2, *Cell Death Differ.* 17 (6) (2010) 994–1002.
- [24] K. Meyerovich, N.M. Violato, M. Fukaya, V. Dirix, N. Pachera, L. Marselli, et al., MCL-1 is a key antiapoptotic protein in human and rodent pancreatic beta-cells, *Diabetes* 66 (9) (2017) 2446–2458.
- [25] L.C. Fogarty, R.T. Flemmer, B.A. Geizer, M. Licursi, A. Karunanithy, J.T. Opferman, et al., Mcl-1 and Bcl-xL are essential for survival of the developing nervous system, *Cell Death Differ.* 26 (8) (2019) 1501–1515.
- [26] X. Wang, M. Bathina, J. Lynch, B. Koss, C. Calabrese, S. Frase, et al., Deletion of MCL-1 causes lethal cardiac failure and mitochondrial dysfunction, *Genes Dev.* 27 (12) (2013) 1351–1364.
- [27] R.L. Thomas, D.J. Roberts, D.A. Kubli, Y. Lee, M.N. Quinsay, J.B. Owens, et al., Loss of MCL-1 leads to impaired autophagy and rapid development of heart failure, *Genes Dev.* 27 (12) (2013) 1365–1377.
- [28] R.M. Percivalle, D.P. Stewart, B. Koss, J. Lynch, S. Milasta, M. Bathina, et al., Antiapoptotic MCL-1 localizes to the mitochondrial matrix and couples mitochondrial fusion to respiration, *Nat. Cell Biol.* 14 (6) (2012) 575–583.
- [29] Y. Liu, Y. Ma, Z. Tu, C. Zhang, M. Du, Y. Wang, et al., Mcl-1 inhibits Mff-mediated mitochondrial fragmentation and apoptosis, *Biochem. Biophys. Res. Commun.* 523 (3) (2020) 620–626.
- [30] A.G. Moyzis, N.S. Lally, W. Liang, L.J. Leon, R.H. Najor, A.M. Orogo, et al., Mcl-1-mediated mitochondrial fission protects against stress but impairs cardiac adaptation to exercise, *J. Mol. Cell. Cardiol.* 146 (2020) 109–120.
- [31] F. Emma, G. Montini, S.M. Parikh, L. Salvati, Mitochondrial dysfunction in inherited renal disease and acute kidney injury, *Nat. Rev. Nephrol.* 12 (5) (2016) 267–280.
- [32] H. Maekawa, T. Inoue, H. Ouchi, T.M. Jao, R. Inoue, H. Nishi, et al., Mitochondrial damage causes inflammation via cGAS-STING signaling in acute kidney injury, *Cell Rep.* 29 (5) (2019) 1261–73 e6.
- [33] A.J. Clark, S.M. Parikh, Mitochondrial metabolism in acute kidney injury, *Semin. Nephrol.* 40 (2) (2020) 101–113.
- [34] K.A. Mapuskar, E.J. Steinbach, A. Zaher, D.P. Riley, R.A. Beardsley, J.L. Keene, et al., Mitochondrial superoxide dismutase in cisplatin-induced kidney injury, *Antioxidants (Basel)* 10 (9) (2021).

- [35] S.J. Han, H.S. Jang, M.R. Noh, J. Kim, M.J. Kong, J.I. Kim, et al., Mitochondrial NADP(+) dependent Isocitrate dehydrogenase deficiency exacerbates mitochondrial and cell damage after kidney ischemia-reperfusion injury, *J. Am. Soc. Nephrol.* 28 (4) (2017) 1200–1215.
- [36] W. Zhang, Y. Yang, H. Gao, Y. Zhang, Z. Jia, S. Huang, Inhibition of mitochondrial complex I aggravates folic acid-induced acute kidney injury, *Kidney Blood Press. Res.* 44 (5) (2019) 1002–1013.
- [37] J. Fan, X. Xu, Y. Li, L. Zhang, M. Miao, Y. Niu, et al., A novel 3-phenylglutaric acid derivative (84-B10) alleviates cisplatin-induced acute kidney injury by inhibiting mitochondrial oxidative stress-mediated ferroptosis, *Free Radic. Biol. Med.* 194 (2022) 84–98.
- [38] Z. Liu, Y. Li, C. Li, L. Yu, Y. Chang, M. Qu, Delivery of coenzyme Q10 with mitochondria-targeted nanocarrier attenuates renal ischemia-reperfusion injury in mice, *Mater. Sci. Eng. C Mater. Biol. Appl.* 131 (2021) 112536.
- [39] Y. Yang, S. Liu, P. Wang, J. Ouyang, N. Zhou, Y. Zhang, et al., DNA-dependent protein kinase catalytic subunit (DNA-PKcs) drives chronic kidney disease progression in male mice, *Nat. Commun.* 14 (1) (2023) 1334.
- [40] Z. Sun, Q. Wang, L. Sun, M. Wu, S. Li, H. Hua, et al., Acetaminophen-induced reduction of NIMA-related kinase 7 expression exacerbates acute liver injury, *JHEP Rep.* 4 (10) (2022) 100545.
- [41] A. Havasi, S.C. Borkan, Apoptosis and acute kidney injury, *Kidney Int.* 80 (1) (2011) 29–40.
- [42] Y. Li, Y. Jiang, W. Zhou, Y. Wu, S. Zhang, G. Ding, et al., Maintaining homeostasis of mitochondria and endoplasmic reticulum with NSC228155 alleviates cisplatin-induced acute kidney injury, *Free Radic. Biol. Med.* 181 (2022) 270–287.
- [43] D.K. Dube, J. Wang, Y. Fan, S. Dube, L. Abbott, J.M. Sanger, et al., Effect of MG-132 on myofibrillogenesis and the ubiquitination of GAPDH in quail myotubes, *Cytoskeleton (Hoboken)* 78 (8) (2021) 375–390.
- [44] A.P. Dennis, D.M. Lonard, Z. Nawaz, B.W. O'Malley, Inhibition of the 26S proteasome blocks progesterone receptor-dependent transcription through failed recruitment of RNA polymerase II, *J. Steroid Biochem. Mol. Biol.* 94 (4) (2005) 337–346.
- [45] Y. Yang, X. Zhan, C. Zhang, J. Shi, J. Wu, X. Deng, et al., USP25-PKM2-glycolysis axis contributes to ischemia reperfusion-induced acute kidney injury by promoting M1-like macrophage polarization and proinflammatory response, *Clin. Immunol.* 109279 (2023).
- [46] J. Pan, J. Zhao, L. Feng, X. Xu, Z. He, W. Liang, Inhibition of USP14 suppresses ROS-dependent ferroptosis and alleviates renal ischemia/reperfusion injury, *Cell Biochem. Biophys.* 81 (1) (2023) 87–96.
- [47] B. Dong, C. Ding, H. Xiang, J. Zheng, X. Li, W. Xue, et al., USP7 accelerates FMR1-mediated ferroptosis by facilitating TBK1 ubiquitination and DNMT1 deubiquitination after renal ischemia-reperfusion injury, *Inflamm. Res.* 71 (12) (2022) 1519–1533.
- [48] Q. Liu, W. Sheng, Y. Ma, J. Zhen, S. Roy, C. Alvira Jafar, et al., USP36 protects proximal tubule cells from ischemic injury by stabilizing c-Myc and SOD2, *Biochem. Biophys. Res. Commun.* 513 (2) (2019) 502–508.
- [49] F. Gao, M. Qian, G. Liu, W. Ao, D. Dai, C. Yin, USP10 alleviates sepsis-induced acute kidney injury by regulating Sirt6-mediated Nrf2/ARE signaling pathway, *J. Inflamm. (Lond.)* 18 (1) (2021) 25.
- [50] J. Huang, Z. Ye, J. Wang, Q. Chen, D. Huang, H. Liu, USP13 mediates PTEN to ameliorate osteoarthritis by restraining oxidative stress, apoptosis and inflammation via AKT-dependent manner, *Biomed. Pharmacother.* 133 (2021) 111089.
- [51] L. Li, J. Wei, S. Li, A.M. Jacko, N.M. Weathington, R.K. Mallampalli, et al., The deubiquitinase USP13 stabilizes the anti-inflammatory receptor IL-1R8/Sigirr to suppress lung inflammation, *EBioMedicine* 45 (2019) 553–562.
- [52] F. Yu, Y. Li, Q. Ye, J. Miao, S.J. Taleb, Y. Zhao, et al., Lipopolysaccharide reduces USP13 stability through c-Jun N-terminal kinase activation in Kupffer cells, *J. Cell. Physiol.* 236 (6) (2021) 4360–4368.
- [53] Z. Wang, L. Jiang, D. Zhang, D. Chen, L. Wang, D. Xiao, USP13-mediated IRAK4 deubiquitination disrupts the pathological symptoms of lipopolysaccharides-induced sepsis, *Microbes Infect.* 23 (9–10) (2021) 104867.
- [54] W. Wang, D. Hu, Y. Feng, C. Wu, Y. Song, W. Liu, et al., Paxillin mediates ATP-induced activation of P2X7 receptor and NLRP3 inflammasome, *BMC Biol.* 18 (1) (2020) 182.
- [55] H. Liu, Z. Zhao, T. Wu, Q. Zhang, F. Lu, J. Gu, et al., Inhibition of autophagy-dependent pyroptosis attenuates cerebral ischaemia/reperfusion injury, *J. Cell. Mol. Med.* 25 (11) (2021) 5060–5069.
- [56] K. Nikhil, K. Shah, The Cdk5-Mcl-1 axis promotes mitochondrial dysfunction and neurodegeneration in a model of Alzheimer's disease, *J. Cell Sci.* 130 (18) (2017) 3023–3039.
- [57] E. Lu, S. Sarkar, J. Raymick, M.G. Paule, Q. Gu, Decreased Mcl-1 protein level in the striatum of 1-methyl-4-phenyl-1,2,3,6-tetrahydropyridine (MPTP)-treated mice, *Brain Res.* 1678 (2018) 432–439.
- [58] X. Cen, Y. Chen, X. Xu, R. Wu, F. He, Q. Zhao, et al., Pharmacological targeting of MCL-1 promotes mitophagy and improves disease pathologies in an Alzheimer's disease mouse model, *Nat. Commun.* 11 (1) (2020) 5731.
- [59] A. Kahraman, J.L. Mott, S.F. Bronk, N.W. Werneburg, F.J. Barreyro, M. E. Guicciardi, et al., Overexpression of mcl-1 attenuates liver injury and fibrosis in the bile duct-ligated mouse, *Dig. Dis. Sci.* 54 (9) (2009) 1908–1917.
- [60] C. Yang, V. Kaushal, S.V. Shah, G.P. Kaushal, Mcl-1 is downregulated in cisplatin-induced apoptosis, and proteasome inhibitors restore Mcl-1 and promote survival in renal tubular epithelial cells, *Am. J. Physiol. Ren. Physiol.* 292 (6) (2007) F1710–F1717.
- [61] Y.C. Ou, C.R. Yang, C.L. Cheng, J.R. Li, S.L. Raung, Y.Y. Hung, et al., Indomethacin causes renal epithelial cell injury involving Mcl-1 down-regulation, *Biochem. Biophys. Res. Commun.* 380 (3) (2009) 531–536.
- [62] L. Liu, C. Yang, C. Herzog, R. Seth, G.P. Kaushal, Proteasome inhibitors prevent cisplatin-induced mitochondrial release of apoptosis-inducing factor and markedly ameliorate cisplatin nephrotoxicity, *Biochem. Pharmacol.* 79 (2) (2010) 137–146.
- [63] N.S. Anstee, C.J. Vandenberg, K.J. Campbell, P.D. Hughes, L.A. O'Reilly, S. Cory, Overexpression of Mcl-1 exacerbates lymphocyte accumulation and autoimmune kidney disease in lpr mice, *Cell Death Differ.* 24 (3) (2017) 397–408.
- [64] Z.K. Zsengeller, L. Ellezian, D. Brown, B. Horvath, P. Mukhopadhyay, B. Kalyanaraman, et al., Cisplatin nephrotoxicity involves mitochondrial injury with impaired tubular mitochondrial enzyme activity, *J. Histochem. Cytochem.* 60 (7) (2012) 521–529.
- [65] Y. Yang, H. Liu, F. Liu, Z. Dong, Mitochondrial dysregulation and protection in cisplatin nephrotoxicity, *Arch. Toxicol.* 88 (6) (2014) 1249–1256.
- [66] M. Zhan, C. Brooks, F. Liu, L. Sun, Z. Dong, Mitochondrial dynamics: regulatory mechanisms and emerging role in renal pathophysiology, *Kidney Int.* 83 (4) (2013) 568–581.
- [67] C. Brooks, Q. Wei, S.G. Cho, Z. Dong, Regulation of mitochondrial dynamics in acute kidney injury in cell culture and rodent models, *J. Clin. Invest.* 119 (5) (2009) 1275–1285.
- [68] J.X. Liu, C. Yang, W.H. Zhang, H.Y. Su, Z.J. Liu, Q. Pan, et al., Disturbance of mitochondrial dynamics and mitophagy in sepsis-induced acute kidney injury, *Life Sci.* 235 (2019) 116828.
- [69] J. Liu, H. Xia, M. Kim, L. Xu, Y. Li, L. Zhang, et al., Beclin1 controls the levels of p53 by regulating the deubiquitination activity of USP10 and USP13, *Cell* 147 (1) (2011) 223–234.
- [70] Z. Gao, C. Li, H. Sun, Y. Bian, Z. Cui, N. Wang, et al., N(6)-methyladenosine-modified USP13 induces pro-survival autophagy and imatinib resistance via regulating the stabilization of autophagy-related protein 5 in gastrointestinal stromal tumors, *Cell Death Differ.* 30 (2) (2023) 544–559.
- [71] B. Lee, Y.H. Kim, W. Lee, H.Y. Choi, J. Lee, J. Kim, et al., USP13 deubiquitinates p62/SQSTM1 to induce autophagy and Nrf2 release for activating antioxidant response genes, *Free Radic. Biol. Med.* 208 (2023) 820–832.
- [72] J. Wang, W. Lin, R. Li, H. Cheng, S. Sun, F. Shao, et al., The deubiquitinase USP13 maintains cancer cell Stemness by promoting FASN stability in small cell lung cancer, *Front. Oncol.* 12 (2022) 899987.
- [73] Q. Yang, W. Lin, Z. Liu, J. Zhu, N. Huang, Z. Cui, et al., RAP80 is an independent prognosis biomarker for the outcome of patients with esophageal squamous cell carcinoma, *Cell Death Dis.* 9 (2) (2018) 146.
- [74] J. Kwon, J. Zhang, B. Mok, C. Han, CK2-mediated phosphorylation upregulates the stability of USP13 and promotes ovarian cancer cell proliferation, *Cancers (Basel)* 15 (1) (2022).
- [75] S. Xiang, J. Fang, S. Wang, B. Deng, L. Zhu, MicroRNA-135b regulates the stability of PTEN and promotes glycolysis by targeting USP13 in human colorectal cancers, *Oncol. Rep.* 33 (3) (2015) 1342–1348.